NATIONAL ADVISORY COMMITTEE FOR AERONAUTICS

TECHNICAL NOTE 3057

A SIMPLIFIED MATHEMATICAL MODEL FOR CALCULATING AERODYNAMIC LOADING AND DOWNWASH FOR WING-FUSELAGE COMBINATIONS WITH WINGS OF ARBITRARY PLAN FORM

By Martin Zlotnick and Samuel W. Robinson, Jr.

Langley Aeronautical Laboratory
Langley Field, Va.

Washington
January 1954

1K

NATIONAL ADVISORY COMMITTEE FOR AERO...

TECHNICAL NOTE 3057

A SIMPLIFIED MATHEMATICAL MODEL FOR CALCULATING AERODYNAMIC LOADING AND DOWNWASH FOR WING-FUSELAGE COMBINATIONS WITH WINGS OF ARBITRARY PLAN FORM[1]

By Martin Zlotnick and Samuel W. Robinson, Jr.

SUMMARY

For the purpose of calculating the aerodynamic loading on the fuselage, the midwing wing-fuselage combination with a fuselage of circular cross section can be represented by a simple system of horseshoe vortices located on the wing with images located inside the fuselage. By using this simplified mathematical model or the extension of it given in an appendix for nonmidwing configurations with fuselages of arbitrary cross section, a method for calculating the lift and longitudinal center of pressure on the fuselage in the presence of the wing at subsonic speeds is presented.

In addition the report shows how the simplified mathematical model can be used for calculating the downwash behind the wing and for calculating the spanwise lift distribution on the wing for midwing configurations with axisymmetric fuselages.

INTRODUCTION

Mutual interference between wing and fuselage has a significant effect on the pitching moment of the wing-fuselage combination, since the longitudinal distribution of the aerodynamic loading on the fuselage is altered by the presence of the wing. Multhopp (ref. 1) has developed a theoretical method for calculating the pitching moment on wing-fuselage combinations with unswept wings which gives good agreement with experimental results. However, for calculating the pitching moment on swept-wing configurations, only semiempirical methods such as that of reference 2 are available.

---

[1]Supersedes the recently declassified NACA RM L52J27a, "A Simplified Mathematical Model for Calculating Aerodynamic Loading and Downwash for Midwing Wing-Fuselage Combinations With Wings of Arbitrary Plan Form" by Martin Zlotnick and Samuel W. Robinson, Jr., 1953.

The aerodynamic loading on the fuselage in subsonic flow is considered in references 1 and 2 to be made up of two parts. The first part, which is due to the fuselage angle of attack resulting from both the geometric angle of attack of the fuselage and the upwash angle induced by the wing, has been calculated in reference 1 for unswept-wing configurations and modified in reference 2 for the swept-wing case. The second part, which is often referred to as the wing lift "carried over" by the fuselage (and which will be referred to in this paper as the "induced lift"), has been calculated analytically for the unswept-wing case in reference 1. However, for swept wings this calculation cannot be applied and no other theoretical method has been available. In reference 2 this component of loading is estimated by an empirical method.

In order to calculate the induced lift on the fuselage in combination with a wing of arbitrary plan form, a method is suggested in the present paper which is based on Lennertz' theoretical work (ref. 3). Lennertz' results, which are concerned only with an unswept lifting line passing through the axis of an infinitely long cylindrical fuselage, are, in effect, generalized so that for midwing configurations in subsonic flow the magnitude, lateral distribution, and longitudinal center of pressure of the induced lift on an axisymmetric fuselage combined with a swept lifting line, or even a lifting surface, can be calculated. An extension of this method to configurations with arbitrary fuselage cross section and wing location is described in appendix A. This extension is based on a result of Flax (ref. 4) and permits the calculation of the magnitude and longitudinal center of pressure of the induced lift, but not its lateral distribution. A numerical example is given in appendix B to illustrate the induced-lift calculations. The effect of finite fuselage length is estimated qualitatively from results of an approximate calculation of the variation with fineness ratio of the induced lift on an ellipsoid of revolution combined with an infinite vortex. The approximate calculation is shown to give results which agree with results of Vandrey (ref. 5).

In calculating the induced lift on the infinitely long fuselage with a circular cross section, the wing-fuselage combination is replaced with a simple system of horseshoe vortices (or doublets) on the wing, with images inside the fuselage. This representation may be used, with some modifications, in calculating the lift on the wing for a midwing configuration with a fuselage of circular cross section and also the corresponding downwash. However, for calculating the downwash and the lift on the wing, the simplified representation of the wing-fuselage combination, although it is considered to be adequate, is no longer rigorous, and the general applicability will depend on experimental verification.

SYMBOLS

A	aspect ratio (wing alone)
a	maximum radius of body of revolution
b	wing span
c	wing chord
$\bar{c}$	mean chord, S/b
c_l	local lift coefficient
d	major axis of ellipsoid of revolution
L_f	total lift on fuselage
m	number of horseshoe vortices
p	static pressure
p_o	free-stream static pressure
q	dynamic pressure
S	wing area (wing alone)
s	semispan of bound leg of horseshoe vortex
U_o	free-stream velocity
U_{max}	maximum longitudinal velocity on surface of body
x_{cp}	longitudinal center of pressure
Γ	vortex strength
ρ	mass density of air
x,y,z	longitudinal, lateral, and vertical ordinates, respectively
u,v,w	longitudinal, lateral, and vertical velocities, respectively
z_h	height of plane of wing above fuselage axis

Subscripts:

a	downwash point
l	on lower surface

n particular pair of horseshoe vortices

u on upper surface

Superscripts:

' dimensionless with respect to a

* dimensionless with respect to b/2

A bar over a symbol denotes that the quantity is dimensionless with respect to s.

BASIC CONSIDERATIONS

Midwing Configurations With Axisymmetric Fuselages

In the major part of the analysis the fuselage is assumed to be an infinite cylinder. To obtain a qualitative estimate of the effect of the finite fuselage length, the variation with fineness ratio of the lift on an ellipsoid of revolution with a wing of infinite span will be calculated approximately in a subsequent section. An approximate method for making the small correction for this effect will be indicated.

Review of results obtained by Lennertz.- Lennertz (ref. 3) has calculated the lateral and longitudinal lift distribution on the fuselage of an idealized wing-fuselage configuration, in which the fuselage is represented by an infinite circular cylinder and the wing by a vortex having constant spanwise circulation. The vortices trailing from the wing tips have images inside the cylinder, and the bound vortex is extended inside the cylinder to join the trailing image vortices as shown in figure 1. With this configuration, the boundary condition of zero velocity normal to the surface of the cylinder is satisfied only at infinity and in the plane normal to the cylinder axis which passes through the vortex, so that it is necessary to superpose an additional potential, which is calculated in reference 3. For this case the lateral lift distribution is obtained by considering the momentum change in a vertical plane infinitely far behind the wing, and the longitudinal lift distribution is obtained by the use of Bernoulli's equation.

Induced lift on infinite cylinder with finite wing having constant spanwise distribution of circulation.- In this section the fuselage lift L_f and its lateral distribution dL_f/dy are shown to be unaffected by the additional potential, so that only the components of L_f and dL_f/dy due to the vortex potential need be calculated.

With all other singularities neglected, the lift on a longitudinal section of the cylinder dy (see fig. 1) due to the vortex potential is calculated as follows:

The pressure p of any point on the surface of the cylinder can be written

$$p = p_o + \frac{1}{2}\rho\left[(U_o + \Delta u)^2 + \Delta v^2 + \Delta w^2\right]$$

where Δu, Δv, and Δw are, respectively, the longitudinal, lateral, and vertical components of velocity induced by the vortices. The section lift dL_f/dy is then written

$$\frac{dL_f}{dy} = \int_{-\infty}^{\infty} (p_u - p_l)dx$$

where p_u and p_l are the pressures on the upper and lower surfaces, respectively. Then

$$\frac{dL_f}{dy} = 2\rho U_o \int_{-\infty}^{\infty} \Delta u \, dx \qquad (1)$$

Only the velocities induced by the bound vortex contribute to the lift.

It may be noted that, since the distribution of the longitudinal velocities induced by the bound vortex is symmetrical about its axis at every section dy, the longitudinal center of pressure of the lift due to the vortex potential is on the axis of the bound vortex.

A closed expression for the integral in equation (1) may be readily derived as follows: Consider the rectangular path indicated by the dashed line in the upper right sketch in figure 1 and the cross section downstream at infinity shown in the lower right sketch of the same figure. The line integral $\oint \Delta u \, ds$ of the tangential velocity component taken around the complete rectangle must be Γ where the path links one of the horseshoe vortices $\left(\left|\frac{a^2}{b/2}\right| < |y| < |a|\right)$, and must be zero where it does not link one of the horseshoe vortices $\left(0 < |y| < \left|\frac{a^2}{b/2}\right|\right)$. Then the desired integral in equation (1), which is the longitudinal

portion of the complete line integral $\oint \Delta u \, ds$, must equal $\oint \Delta u \, ds$ minus the line integral along the short vertical line at infinity $\int_u^l \Delta w(\infty,y,z)dz$, where u refers to the upper surface and l refers to the lower surface. That is,

$$2\int_{-\infty}^{\infty} \Delta u \, dx = \oint \Delta u \, ds - \int_u^l \Delta w(\infty,y,z)dz \tag{2}$$

Since

$$\Delta w = -\frac{\partial \phi}{\partial z}$$

then

$$\int_u^l \Delta w \, dz = \phi_u - \phi_l$$

where ϕ_u and ϕ_l are the potentials on the upper and lower surfaces, respectively, in the plane $x = \infty$. When $\left|\frac{a^2}{b/2}\right| < |y| < |a|$,

$$\phi_u = -\phi_l$$

$$= \frac{\Gamma}{2\pi}\left(\tan^{-1}\frac{\sqrt{a^2 - y^2}}{y - \frac{b}{2}} - \tan^{-1}\frac{\sqrt{a^2 - y^2}}{y + \frac{b}{2}} - \tan^{-1}\frac{\sqrt{a^2 - y^2}}{y - \frac{a^2}{b/2}} + \tan^{-1}\frac{\sqrt{a^2 - y^2}}{y + \frac{a^2}{b/2}}\right)$$

$$= \frac{1}{\pi}\Gamma \tan^{-1}\frac{2\frac{b}{2}\sqrt{a^2 - y^2}}{\left(\frac{b}{2}\right)^2 - a^2}$$

and

$$\oint \Delta u \, ds = \Gamma$$

and when $0 < |y| < \left|\frac{a^2}{b/2}\right|$ the strength of the image vortex located at $\frac{a^2}{b/2}$ is increased by π:

$$\phi_u = -\phi_l$$

$$= \frac{\Gamma}{2\pi}\left[\tan^{-1}\frac{\sqrt{a^2-y^2}}{y-\frac{b}{2}} - \tan^{-1}\frac{\sqrt{a^2-y^2}}{y+\frac{b}{2}} - \left(\pi + \tan^{-1}\frac{\sqrt{a^2-y^2}}{y-\frac{a^2}{b/2}}\right) + \tan^{-1}\frac{\sqrt{a^2-y^2}}{y+\frac{a^2}{b/2}}\right]$$

$$= \frac{1}{\pi}\Gamma\left[\tan^{-1}\frac{2\frac{b}{2}\sqrt{a^2-y^2}}{\left(\frac{b}{2}\right)^2 - a^2} - \frac{\pi}{2}\right]$$

and

$$\oint \Delta u \, ds = 0$$

Then, from equation (2), the lateral lift distribution of the induced lift can be written

$$\frac{dL_f}{dy} = \rho U_o \Gamma\left[1 - \frac{2}{\pi}\tan^{-1}\frac{2\frac{b}{2}\sqrt{a^2-y^2}}{\left(\frac{b}{2}\right)^2 - a^2}\right] \qquad (-a < y < a) \qquad (3)$$

and after integration over y,

$$L_f = 2\rho U_o \Gamma\left(a - \frac{a^2}{b/2}\right) \qquad (4)$$

These expressions are the same, except for the difference in notation, as the expressions obtained in reference 3 for dL_f/dy and the total fuselage lift L_f. The components of L_f and dL_f/dy due to the additional potential must therefore be zero.

The longitudinal lift distribution on the cylinder calculated in reference 3, which includes the effect of the additional potential as well as the vortex potential, is slightly different from that which would be calculated by taking into account the effect of the vortex potential alone. However, both distributions are symmetrical about the axis of the bound vortex. The longitudinal center of pressure of the lift due to the vortex potential must be at the bound-vortex axis because the longitudinal velocities induced on the surface of the cylinder by the bound vortex are the same in front and in back of the bound vortex, as noted previously. That the longitudinal center of pressure of the lift due to the vortex potential and the additional potential must be at the axis of the bound vortex is indicated by the calculations of reference 3 (although not explicitly stated) and can be shown as follows:

Superposition of infinite vortices canceling the semi-infinite trailing vortices of figure 2(a) as shown in figure 2(b) will not change the longitudinal lift distribution on the cylinder, since no longitudinal velocities are induced. It is apparent that the system is the same as before, with the direction of the trailing legs of the horseshoe vortices reversed; therefore, the longitudinal distribution on the infinite cylinder must be symmetrical about the axis of the bound vortex, since, if it were not, the longitudinal lift distributions on the cylinders in figures 2(a) and 2(b) would be different.

From the analysis in this section of the wing and cylinder combination it can be seen that, for calculating the lift on the cylinder, its lateral distribution, and the longitudinal center of pressure, only the effect of the vortex potential need be considered. This lift due to the vortex potential will be referred to hereinafter as the "induced lift."

Simplified representation of wing-fuselage combination.- In this paper, the wing-fuselage combination will be represented by a system of discrete horseshoe vortices and images, so that configurations with wings of arbitrary plan form may be treated. It is necessary to superpose two pairs of horseshoe vortices of the types shown in figures 1 and 3 to obtain the vortex-image system of figure 4. The vortex-image system of figure 4 can be used to represent wings of arbitrary plan form in the manner shown in figure 5 by locating the bound vortices on the wing quarter-chord line or by distributing them over the wing surface. Since the discrete horseshoe vortex becomes a doublet line as the length of the bound leg approaches zero, it is also possible to represent the wing by a continuous distribution of doublets.

Figure 3 shows the larger pair of vortices with span $2(y_n + s)$ and strength $+\Gamma$ near the smaller pair of span $2(y_n - s)$ and strength $-\Gamma$. When the bound legs of the smaller are moved to coincide with the bound legs of the larger, the net vortex strength along the

section where they coincide is zero, and the remaining sections of the larger bound legs form the bound legs of the desired system (see fig. 4). From equations (3) and (4), the lateral distribution of the induced lift and the total induced lift for the vortex-image system shown in figure 4 are given by the following expressions:

$$\frac{\Delta\left(\frac{dL_f}{dy}\right)}{q\bar{c}} = \left(\frac{cc_l}{\bar{c}}\right)_n \frac{2}{\pi}\left[\tan^{-1}\frac{2(y_n - s)\sqrt{a^2 - y^2}}{(y_n - s)^2 - a^2} - \tan^{-1}\frac{2(y_n + s)\sqrt{a^2 - y^2}}{(y_n + s)^2 - a^2}\right] \tag{5}$$

$$\frac{\Delta L_f}{qS} = \left(\frac{cc_l}{\bar{c}}\right)_n s^* \frac{2a^2}{y_n^2 - s^2} \tag{6}$$

where $\left(\frac{cc_l}{\bar{c}}\right)_n$ is the loading coefficient on the wing at the station y_n.

Since it is known that the longitudinal center of pressure of the induced lift for each pair of horseshoe vortices and images is still located at the axis of the bound vortex, it is possible by superposition to calculate the pitching moment on the fuselage in the presence of a wing of arbitrary plan form if the lift distribution on the wing is known, although the complete longitudinal lift distribution cannot be calculated unless the component of loading due to the additional potential is calculated. The total induced lift and its lateral lift distribution can also be calculated by superposition. The method for calculating the total induced lift and its lateral distribution and longitudinal center of pressure is discussed in a subsequent section, and an illustrative example is given in appendix B.

Effect of Finite Fuselage Length on Induced Lift

In order to obtain an estimate of the error involved in the assumption of the foregoing analysis that the fuselage is infinitely long, an approximate calculation will be made of the effect of fineness ratio on the induced lift of an ellipsoid of revolution combined with an infinite vortex. The limiting case of the spherical fuselage is treated first in the manner of Vandrey (ref. 5), and then the general case is treated.

Lift on a combination of sphere and infinite vortex.- The potential of the sphere combined with an infinite vortex (fig. 6(a)) is written

$$\phi = \frac{\Gamma}{2\pi} \tan^{-1} \frac{z}{x} + U_o x \left[1 + \frac{1}{2} \frac{a^3}{\left(\sqrt{x^2 + y^2 + z^2} \right)^3} \right] \tag{7}$$

where the potential for the sphere in the free stream is

$$\phi_1 = U_o x \left[1 + \frac{1}{2} \frac{a^3}{\left(\sqrt{x^2 + y^2 + z^2} \right)^3} \right] \tag{8}$$

and the potential for the vortex is

$$\phi_2 = \frac{\Gamma}{2\pi} \tan^{-1} \frac{z}{x} \tag{9}$$

The lift on a section of the sphere in the plane $y = \text{Constant}$ is

$$\frac{dL_f}{dy} = \int_{-\sqrt{a^2-y^2}}^{\sqrt{a^2-y^2}} (p_u - p_l) dx \tag{10}$$

where p_u and p_l are the pressures on the upper and lower surfaces, respectively. From Bernoulli's equation,

$$p = p_o + \frac{1}{2}\rho \left[(u + \Delta u)^2 + (v + \Delta v)^2 + (w + \Delta w)^2 \right] \tag{11}$$

and

$$p_u - p_l = 2\rho(u \, \Delta u + w \, \Delta w)$$

where Δu, Δv, and Δw are the velocities induced by the vortex on the upper half of the sphere and u, v, and w are the local velocities on the surface of the sphere. Thus

$$\left.\begin{aligned} \Delta u &= \frac{\Gamma}{2\pi}\frac{z}{a^2 - y^2} \qquad \Delta w = \frac{\Gamma}{2\pi}\frac{x}{a^2 - y^2} \\ u &= \frac{3}{2}U_o\frac{a^2 - x^2}{a^2} \qquad w = \frac{3}{2}U_o\frac{xz}{a^2} \end{aligned}\right\} \tag{12}$$

The lift on the section at y = Constant is

$$\frac{dL_f}{dy} = \frac{3}{2}\frac{\Gamma}{\pi}\frac{\rho U_o}{a^2 - y^2}\int_{-\sqrt{a^2-y^2}}^{\sqrt{a^2-y^2}} z\,dx \tag{13}$$

which may be written in the form

$$\frac{dL_f}{dy} = \rho U_{max}\int_{-f(y)}^{f(y)} 2\,\Delta u\,dx \tag{14}$$

since

$$\Delta u = \frac{\Gamma}{2\pi}\frac{z}{a^2 - y^2}$$

and since

$$u = U_{max}$$

when $x = 0$, so that

$$U_{max} = \frac{3}{2}U_o$$

For an infinite cylinder with an infinite vortex, equation (14) will also hold. In this case

$$U_{max} = U_o$$

$$\Delta u = \frac{\Gamma}{2\pi} \frac{\sqrt{a^2 - y^2}}{a^2 - y^2 + x^2}$$

and

$$f(y) = \infty$$

From equation (13) or (14) the lift obtained for the sphere is

$$\frac{dL_f}{dy} = \frac{3}{4} \rho U_o \Gamma$$

and for the cylinder

$$\frac{dL_f}{dy} = \rho U_o \Gamma$$

Equation (14) gives the exact result for the case of the sphere with an infinite vortex and the same result as the method of reference 3 for the case of an infinite cylinder with an infinite vortex. Therefore, equation (14) presumably would give a qualitative estimate for the intermediate case of an ellipsoid of revolution having a fineness ratio between 1 and infinity. This assumption is made in the following section and the value obtained for the induced lift by using equation (14) is shown to be very close to that obtained by the more accurate mathematical treatment of Vandrey (ref. 5) for the case of an ellipsoid having a fineness ratio of 5.

Lift on a combination of ellipsoid and infinite vortex.- The local lift on the ellipsoid is given by equation (14):

$$\frac{dL_f}{dy} = \rho U_{max} \int_{-f(y)}^{f(y)} 2 \Delta u \, dx$$

From figure 6(b),

$$f(y) = d\sqrt{1 - \left(\frac{y}{a}\right)^2} \tag{15}$$

$$\Delta u = \frac{\Gamma}{2\pi} \frac{a\sqrt{1 - \left(\frac{y}{a}\right)^2 - \left(\frac{x}{d}\right)^2}}{x^2 + a^2\left[1 - \left(\frac{y}{a}\right)^2 - \left(\frac{x}{d}\right)^2\right]} \tag{16}$$

The integration indicated in equation (14) yields

$$\frac{1}{\rho U_o \Gamma} \frac{dL_f}{dy} = \frac{U_{max}/U_o}{1 + \frac{a}{d}} \tag{17}$$

The values of U_{max}/U_o given as a function of the fineness ratio in reference 6 are shown in figure 7.

Figure 8 shows a plot of $\frac{1}{\rho U_o \Gamma} \frac{dL_f}{dy}$ against d/a. The result of a calculation from reference 5 for the case of an ellipsoid with $\frac{d}{a} = 5$ falls near the curve in figure 8. Since the calculations of reference 5 appear to be accurate to 0.05, the agreement may be even better than is indicated in figure 8. The results of reference 5 are obtained by difficult computations for each body separately, and the method does not yield a general expression similar to equation (17).

Figure 8 indicates that the induced lift on the ellipsoids having high fineness ratios $\left(\frac{d}{a} > 5\right)$ is about 90 percent of the induced lift on the infinite cylinder. Since the fuselage is similar in effect to a semi-infinite cylinder because of the wake which extends behind it, the loss in lift due to the finite fuselage length is about half of that indicated by the calculation for the ellipsoid of revolution. The value of induced lift obtained by assuming the fuselage to be an infinite cylinder may be multiplied by the factor $\frac{1}{2}\left(1 + \frac{U_{max}/U_o}{1 + \frac{a}{d}}\right)$ to correct for the finite fuselage length in the presence of an infinite wing; however, this approximate correction can often be neglected since it is nearly unity for most practical fineness ratios. Since the correction is small, it is assumed that it may be applied directly for the finite-wing case without introducing significant error, so that the factor $\frac{1}{2}\left(1 + \frac{U_{max}/U_o}{1 + \frac{a}{d}}\right)$ is to be multiplied by equations (5) and (6) to correct for finite fuselage length.

APPLICATION OF SIMPLIFIED MATHEMATICAL MODEL TO CALCULATION OF AERODYNAMIC LOADING AND DOWNWASH

In the following sections, the method for calculating the induced lift will be described and discussed, and methods for calculating the spanwise loading on the wing and the downwash will be outlined. The methods for calculating the downwash and spanwise lift distribution are not rigorous since the effect of the additional potential, which has not yet been calculated, must be approximated by a simple correction. Although the validity of the correction must depend on experimental verification, it is believed to be adequate, and the exact value of the additional potential may be incorporated into the method immediately when it is calculated.

Method for Calculating Induced Lift on Fuselage

If the lift distribution on the wing in the presence of the fuselage is known, say from reference 7 (see fig. 9) or the method outlined in the following section, the induced lift may be calculated very simply. For midwing configurations with fuselages of circular cross section, equations (5) and (6) are used to calculate the magnitude of the induced lift, its lateral distribution, and its longitudinal center of pressure, as shown in appendix B. For configurations with arbitrary cross section and wing location, the results of appendix A must be used. The method of appendix A, however, will not give the lateral distribution of the induced lift.

A sample numerical calculation is shown in appendix B for the midwing configuration with the circular fuselage. It is necessary only to substitute into equations (5) and (6) the value of loading coefficient $\frac{cc_l}{\bar{c}}$ for each of the discrete horseshoe vortices. The values of the increments of the lateral lift distributions $\Delta \frac{dL_f}{dy}$ on the fuselage due to all of the horseshoe vortices and their images obtained from equation (5) are superposed to get the complete lateral lift distribution dL_f/dy. The increment of total lift ΔL_f for each pair of horseshoe vortices and images acts at the bound-vortex axis, and the longitudinal center of pressure of the total lift L_f is obtained simply by dividing the sum of the moments of the incremental total lifts ΔL_f by the total lift L_f (the sum of the increments ΔL_f).

In calculating the longitudinal center of pressure of the induced lift, the bound legs of the wing horseshoe vortices should be located at the section center of pressure. Since the present methods do not

provide a means for calculating the chordwise lift distribution on the wing in the presence of the fuselage, the section centers of pressure were assumed to lie on the wing quarter-chord line as in approximate calculations of the aerodynamic center of the wing alone. However, a better approximation to the longitudinal center of pressure of the induced lift may be obtained by assuming that near the wing-fuselage juncture and near the wing tip the spanwise variation of the section center-of-pressure location is the same as that near the root and tip of the wing alone as determined from measurements or lifting-surface calculations. Curves in reference 8 showing the spanwise variation of section center of pressure for several wing plan forms may serve as a guide for estimating the wing-alone values to be used in preliminary calculations.

The results of the calculation for the lateral distribution of induced lift and the longitudinal center of pressure carried out in appendix B are presented in figures 10 and 11, respectively. Figure 11 shows the increment of total lift ΔL_f contributed by each pair of vortices and images and it can be seen that the contribution to the total lift L_f due to the outboard part of the wing (the components farthest to the right in the figure) is small compared with the contribution of the inboard part of the wing. The induced lift on the fuselage has also been calculated by using the wing-alone spanwise lift distribution shown in figure 9; that is, the effect of the fuselage on the wing is neglected. It can be seen in figures 10 and 11 that, although there is about a 10-percent increase in the magnitude of dL_f/dy and L_f due to the effect of the fuselage on the wing, the lateral and longitudinal load distribution on the fuselage is practically unaffected. The correction for finite length has not been included in the calculations. This correction would decrease the magnitude of the lift, but it would not alter the lateral or longitudinal distribution.

The total lift and moment on the fuselage can be obtained by adding the components of lift and moment due to the induced lift to the components of lift and moment due to the local angle of attack of the fuselage (which can be calculated as shown in ref. 2). The lift and moment on the part of the wing outboard of the fuselage, calculated by the method of reference 7 or the method of this paper (described in a subsequent section), may then be added to the lift and moment on the fuselage to get the total lift and moment on the combination.

Outline of Method for Calculating Lift on Wing in Presence of Fuselage

The lift distribution on the wing will be calculated by equating the downwash angle induced at the three-quarter-chord line by the horseshoe vortices centered on the quarter-chord line (see fig. 5) to the local angle of attack on the three-quarter-chord line at several points along the span. Since the boundary conditions on the fuselage are not completely satisfied by the vortex-image system of figure 5 in the region near the bound vortex, it is necessary to resort to certain approximations in calculating the downwash. Calculation of the exact values of these downwash functions would require the calculation of the additional potential, which involves a great deal of time and effort, but if such calculations were made the values could be used directly in the present method and the restrictions suggested in the following paragraph would be eliminated.

The approximations described in the following sections improve as the longitudinal distance from the downwash points to the bound vortex increases, so that this method is considered to be best suited for configurations having a fairly small ratio of diameter to root chord, say for straight wings with $\frac{\text{Diameter}}{\text{Root chord}} \leqq \frac{1}{2}$ and for swept wings with $\frac{\text{Diameter}}{\text{Root chord}} \leqq \frac{1}{3}$. Calculations of the aerodynamic loading on a wing and tip-tank combination, by a method corresponding to the one described herein with the downwash points located about 1 tip-tank diameter behind the bound vortex $\left(\frac{\text{Diameter}}{\text{Tip chord}} \approx \frac{1}{2}\right)$, have been found to yield results in good general agreement with experimental results (ref. 9).

Downwash near bound vortex of wing.- Although the boundary conditions are satisfied completely only at infinity, the trailing legs of a single pair of horseshoe vortices and images also satisfy the boundary conditions on the cylinder in the plane perpendicular to the cylinder axis which passes through the bound legs of the horseshoe vortices. In addition, the boundary conditions on the cylinder are satisfied completely by the semi-infinite vortex-image system everywhere in the plane of the horseshoe vortex. Since the boundary conditions on the cylinder are satisfied exactly at the points noted, and are partly satisfied everywhere else, it will be assumed that the downwash due to the trailing vortices may be calculated approximately, at least in the plane of the horseshoe vortex, without introducing any correction factor.

However, a correction factor must be used in calculating the downwash due to the real and image bound vortices which have the greatest tendency to violate the boundary condition of zero velocity normal to

the surface of the cylinder. In the plane of the wing, along a line parallel to the bound vortex, the effect of the cylinder on the vertical flow induced by the bound vortex is assumed to be the same as its effect on a two-dimensional uniform rectilinear flow, so that the downwash induced by the bound vortices on that line is increased by the factor $1 + \frac{a^2}{y_a^2}$.

The downwash angle at a point $y = y_a$ and $x = x_a$ (shown in fig. 4) is then written

$$\alpha_a = \frac{1}{4\pi A}\frac{b}{2s}\sum_n \left(\frac{cc_l}{\bar{c}}\right)_n \left[F_n(x,y,0) + G_n(x,y,0)\left(1 + \frac{a^2}{y_a^2}\right)\right] \tag{18}$$

where the downwash factor due to the trailing vortices F_n and the downwash factor due to the bound vortices G_n may be calculated by the Biot-Savart law.

The function F_n is the sum of four terms, each having the form

$$\frac{1}{\bar{y}_n - \bar{y}_a + 1}\left[\frac{\bar{x}_a - \bar{x}_n}{\sqrt{(\bar{y}_n - \bar{y}_a + 1)^2 + (\bar{x}_a - \bar{x}_n)^2}} + 1\right] -$$

$$\frac{1}{\bar{y}_n - \bar{y}_a - 1}\left[\frac{\bar{x}_a - \bar{x}_n}{\sqrt{(\bar{y}_n - \bar{y}_a - 1)^2 + (\bar{x}_a - \bar{x}_n)^2}} + 1\right]$$

(the term corresponding to the trailing legs of the horseshoe vortex centered at $y = y_n$), and the function G_n is the sum of four terms, each having the form

$$\frac{1}{\bar{x}_a - \bar{x}_n}\left[\frac{\bar{y}_n - \bar{y}_a + 1}{\sqrt{(\bar{y}_n - \bar{y}_a + 1)^2 + (\bar{x}_a - \bar{x}_n)^2}} - \frac{\bar{y}_n - \bar{y}_a - 1}{\sqrt{(\bar{y}_n - \bar{y}_a - 1)^2 + (\bar{x}_a - \bar{x}_n)^2}}\right]$$

(the term corresponding to the bound leg of the horseshoe vortex centered at $y = y_n$).

Scheme for calculating spanwise lift distribution on wing.- The lift distribution on the wing is calculated by equating the downwash angle on the wing induced by the vortex-image system to the local angle of attack on the three-quarter-chord line of the wing at m points as in reference 7. Thus equation (18) is written for each of the m stations, and the simultaneous equations can then be solved for $\left(\frac{cc_l}{\bar{c}}\right)_n$ at m points on the span. The + marks in figure 5 indicate the points where the downwash is equated to the local angle of attack.

The effective angle of attack α_a is equal to the geometric angle of attack of the wing α_g plus the angle of attack induced by the fuselage:

$$\alpha_a = \alpha_g + \alpha_f' \tag{19}$$

and

$$\alpha_f' = \alpha_f\left(1 + \frac{a^2}{y_a^2}\right) - \alpha_f$$

$$= \alpha_f \frac{a^2}{y^2} \tag{20}$$

where α_f is the geometric angle of attack of the fuselage and the factor $1 + \frac{a^2}{y_a^2}$ takes into account the increase in the vertical velocity of the free stream in the neighborhood of the fuselage as calculated by assuming the fuselage to be an infinite cylinder in a two-dimensional uniform rectilinear flow of magnitude $U_o\alpha_f$.

The effect of finite fuselage length (referred to in ref. 7 as the "inflow effect") must be included separately by multiplying $\frac{cc_l}{\bar{c}}$ at each spanwise station by the factor $1 + 2\epsilon$, where ϵ is the ratio of the local increment of longitudinal velocity due to the fuselage to the free-stream velocity. As shown in reference 7, the factor $1 + 2\epsilon$ is used to account approximately for the small increase in dynamic pressure of the flow over the wing due to the increase in the local longitudinal velocity near the surface of a fuselage of finite length.

Outline of Method for Calculating Downwash

The downwash calculations made in this section are for the case of the wing at an angle of incidence with the fuselage at zero geometric angle of attack. The accuracy of the calculated results must be verified by experimental results; however, by comparison with results of downwash calculations for the wing alone, the results of the calculations for the downwash behind the wing-fuselage combination may serve to give useful information regarding the effect of the wing-fuselage interference.

As was noted previously, the boundary conditions on the wing-fuselage combination are completely satisfied by the vortex-image system infinitely far behind the wing. At a great distance behind the wing, therefore, the theoretical value of the downwash can be calculated accurately for a given spanwise lift distribution. This calculation is simple, and the results may be useful for certain applications. However, the approximations made in the preceding section for calculating the downwash at the wing three-quarter-chord line may give more accurate results for the downwash in the plane of the wing in the region nearer the bound vortex.

If the lift distribution on the wing is known, say from the method of reference 7 or the method outlined in this paper, the downwash angle in the plane $x = \infty$ may be calculated by adding the downwash due to each pair of trailing vortices and their images. Thus, from the Biot-Savart law and figure 4, the downwash angle α_a at the point $y = y_a$, $z = z_a$, and $x = \infty$ is given as

$$\alpha_a = \frac{1}{2\pi A s^*} \sum_n \left(\frac{cc_l}{\bar{c}}\right)_n F_n \tag{21}$$

where

$$F_n = \frac{\bar{y}_n - \bar{y}_a + 1}{(\bar{y}_n - \bar{y}_a + 1)^2 + \bar{z}_a^2} - \frac{\bar{y}_n - \bar{y}_a - 1}{(\bar{y}_n - \bar{y}_a - 1)^2 + \bar{z}_a^2} + \frac{\bar{y}_n + \bar{y}_a + 1}{(\bar{y}_n + \bar{y}_a + 1)^2 + \bar{z}_a^2} -$$

$$\frac{\bar{y}_n + \bar{y}_a - 1}{(\bar{y}_n + \bar{y}_a - 1)^2 + \bar{z}_a^2} + \frac{\bar{y}_a - \frac{\bar{a}^2}{\bar{y}_n} + 1}{\left(\bar{y}_a - \frac{\bar{a}^2}{\bar{y}_n} + 1\right)^2 + \bar{z}_a^2} - \frac{\bar{y}_a - \frac{\bar{a}^2}{\bar{y}_n} - 1}{\left(\bar{y}_a - \frac{\bar{a}^2}{\bar{y}_n} - 1\right)^2 + \bar{z}_a^2} +$$

$$\frac{\bar{y}_a + \frac{\bar{a}^2}{\bar{y}_n} + 1}{\left(\bar{y}_a + \frac{\bar{a}^2}{\bar{y}_n} + 1\right)^2 + \bar{z}_a^2} - \frac{\bar{y}_a + \frac{\bar{a}^2}{\bar{y}_n} - 1}{\left(\bar{y}_a + \frac{\bar{a}^2}{\bar{y}_n} - 1\right)^2 + \bar{z}_a^2} \tag{22}$$

and $(cc_l/\bar{c})_n$ is the loading coefficient at station $\pm y_n$.

The representation of the wake by discrete vortices is satisfactory if the downwash is calculated at points halfway between the trailing legs ($y_a = y_n$). The values calculated at these points may be faired to obtain a continuous spanwise distribution of downwash angle.

CONCLUDING REMARKS

For the purpose of calculating the longitudinal loading on the fuselage in subsonic flow, a midwing wing-fuselage combination with a fuselage of circular cross section has been represented by a system of discrete horseshoe vortices and images. By using this simplified mathematical model, or the extension of it given in an appendix for nonmidwing configurations with fuselages of arbitrary cross section, a method is derived for calculating the lift on the fuselage induced by the wing. The method is illustrated by a numerical example. This "induced lift" can be added to the lift on the part of the wing outboard of the fuselage and the lift on the fuselage due to the upwash induced by the wing to get the total loading on the wing-fuselage combination.

In addition to the method for calculating the induced lift, which is theoretically rigorous, methods for calculating the downwash far behind the wing and for calculating the spanwise lift distribution on the wing for midwing configurations with axisymmetric fuselages are outlined. In calculating the spanwise lift distribution on the wing, approximations are made to account for the effect of the "additional potential," so that the method is not rigorous. However, the effect of the additional potential may easily be incorporated into the method when it is calculated.

Langley Aeronautical Laboratory,
National Advisory Committee for Aeronautics,
Langley Field, Va., November 13, 1952.

APPENDIX A

CALCULATION OF INDUCED LIFT FOR CONFIGURATIONS WITH ARBITRARY CROSS SECTION AND WING LOCATION

This appendix indicates how the relation, given in reference 4, between the magnitude of the induced lift on a cylindrical fuselage and the lift distribution on the wing can be generalized so that a simple equation can be obtained from which the longitudinal center of pressure of the induced lift may be calculated. Reference 4 shows that the following relation will hold between the total lift induced on a cylindrical fuselage of arbitrary cross section and the lift distribution on a wing in the horizontal plane $z = \text{Constant}$:

$$L_f = \int_W \rho U_o \Gamma(y) g(y) dy \tag{A1}$$

where y is the lateral ordinate, $\Gamma(y)$ is the spanwise distribution of circulation, $g(y)$ is the increment in the flow velocity normal to the plane of the wing produced by a unit uniform transverse flow normal to the cylinder axis, and W indicates that the integral is taken over the span of the exposed wing.

In order to generalize equation (A1) so that the center of pressure of the induced lift on the fuselage can be calculated, it is convenient to consider wing elements to be represented by horseshoe vortices having bound legs of vanishingly small length δy_n lying in the horizontal plane $z = \text{Constant}$ with trailing legs parallel to the x-axis (longitudinal axis). On a cylinder having its axis coinciding with the x-axis, these horseshoe vortices will each induce a lift of magnitude δL_f, defined by

$$\delta L_f = \int_{y_n - \delta y_n}^{y_n + \delta y_n} \rho U_o \Gamma(y) g(y) dy \tag{A2}$$

where y_n is the lateral location of the center of the bound leg. It can be shown that the longitudinal location of the center of pressure of this induced lift δL_f is at x_n, the same longitudinal location as the bound leg of the horseshoe vortex. The proof is exactly the same in all essentials as that presented in the body of this paper for the case of a circular cylinder with a finite horseshoe vortex located in the plane $z = 0$.

From these considerations, it is clear that the total induced lift on the fuselage and its longitudinal center of pressure x_{cp} can be given as follows:

$$L_f = \rho U_o \int_S \gamma(x,y)g(y)dS \tag{A3a}$$

$$x_{cp} = \frac{\rho U_o \int_S x\gamma(x,y)g(y)dS}{L_f} \tag{A3b}$$

where $\gamma(x,y)$ is the strength of an infinitesimal horseshoe vortex centered at (x,y), and the integrals are to be taken over the exposed wing surface S. It may be noted that, whereas equation (A3a) is valid at all subsonic and supersonic Mach numbers, equation (A3b) is valid only at subsonic Mach numbers.

Equations (A3a) and (A3b) represent, in general, the desired equations for the magnitude and center of pressure of the induced lift on a cylinder in the presence of a lifting surface. In order to illustrate their application, they will be developed for the case of a circular fuselage with a lifting line of horseshoe vortices and will be reduced so that the simple computational procedure of appendix B can be used.

For a circular cylinder of radius a, $g(y)$ is given as

$$g(y) = \frac{a^2(y^2 - z^2)}{(y^2 + z^2)^2}$$

When the wing is represented by a lifting line, equation (A3a) has the same form as equation (A2) and the increment in lift ΔL_f due to two horseshoe vortices of strength Γ having spans $2s$ and located in the horizontal plane $z = z_h$ at $+y_n$ and $-y_n$ is

$$\Delta L_f = 2\rho U_o \Gamma \int_{y_n-s}^{y_n+s} \frac{a^2(y^2 - z_h^2)}{(y^2 + z_h^2)^2}\, dy$$

$$= 2qS\left(\frac{cc_l}{\bar{c}}\right)_n a^2 s^* \frac{y_n^2 - s^2 - z_h^2}{z_h^4 + 2z_h^2(y_n^2 + s^2) + (y_n^2 - s^2)^2} \tag{A4}$$

It may be noted that for the midwing case $z_h = 0$, equation (A4) is identical to equation (6).

APPENDIX B

ILLUSTRATIVE EXAMPLE OF INDUCED-LIFT CALCULATION

A numerical example is given to illustrate the method presented in the body of the paper for calculating the induced lift on the fuselage.

Geometric Characteristics of Configuration Used in Illustrative Example

The plan view of the wing-fuselage combination is essentially the same as shown in figure 5. The geometric data are:

Aspect ratio	8
Taper ratio	0.45
Sweepback, deg	45
a*	0.10
s*	0.05

Spanwise Loading on Wing in Presence of Fuselage

The spanwise lift distribution on the wing in the presence of the fuselage for a high-midwing configuration, tabulated below and shown in figure 9, was obtained by the method of reference 7. It is qualitatively correct for the pure midwing case and is used to illustrate the procedure for obtaining the induced lift on the fuselage and its lateral distribution and longitudinal center of pressure. The lift distribution on the wing in the presence of the fuselage, plotted in figure 9, is tabulated as follows:

n	y_n^*	x_n^*	$\left(\frac{cc_l}{\bar{c}}\right)_n$
1	0.15	0.15	0.369
2	.25	.25	.366
3	.35	.35	.356
4	.45	.45	.338
5	.55	.55	.319
6	.65	.65	.300
7	.75	.75	.266
8	.85	.85	.241
9	.95	.95	.200

Longitudinal Distribution of Induced Lift

Equation (6), which gives the lift on the fuselage due to a single pair of horseshoe vortices at $(x_n', \pm y_n')$ and their images, can be written

$$\frac{\Delta L_f}{qS} = \left(\frac{cc_l}{\bar{c}}\right)_n s^* \frac{2}{y_n'^2 - s'^2} \tag{B1}$$

The total lift L_f/qS is then

$$\frac{L_f}{qS} = s^* \sum_n \left(\frac{cc_l}{\bar{c}}\right)_n \frac{2}{y_n'^2 - s'^2} \tag{B2}$$

The longitudinal center of pressure referred to the intersection of the quarter-chord line and the fuselage axis of symmetry (see fig. 5) is

$$x_{cp}' = \frac{\sum_n \left(\frac{cc_l}{\bar{c}}\right)_n \frac{2}{y_n'^2 - s'^2} x_n'}{\sum_n \left(\frac{cc_l}{\bar{c}}\right)_n \frac{2}{y_n'^2 - s'^2}} \tag{B3}$$

The computed values of L_f/qS and x_{cp}' are obtained from the values presented in the following table:

n	$\frac{2}{y_n'^2 - s'^2}$	$\left(\frac{cc_l}{\bar{c}}\right)_n \frac{2}{y_n'^2 - s'^2}$	$\left(\frac{cc_l}{\bar{c}}\right)_n \frac{2}{y_n'^2 - s'^2} x_n'$
1	1.000	0.369	0.554
2	.333	.122	.305
3	.168	.060	.210
4	.100	.034	.153
5	.066	.021	.116
6	.048	.014	.091
7	.036	.010	.075
8	.028	.007	.060
9	.022	.005	.048
		$\sum$ = 0.642	$\sum$ = 1.612

$$\frac{L_f}{qS} = 0.05 \sum_{1}^{9} \left(\frac{cc_l}{\bar{c}}\right)_n \frac{2}{y_n'^2 - s'^2} = 0.032$$

$$x_{cp}' = \frac{\sum_{1}^{9} \left(\frac{cc_l}{\bar{c}}\right)_n \frac{2}{y_n'^2 - s'^2} x_n'}{\sum_{1}^{9} \left(\frac{cc_l}{\bar{c}}\right)_n \frac{2}{y_n'^2 - s'^2}} = 2.51$$

The values of $s^*\left(\frac{cc_l}{\bar{c}}\right)_n \frac{2}{y_n'^2 - s'^2}$ are plotted as vectors in figure 11. The location of x_{cp}' is also shown.

Lateral Distribution of Induced Lift

Equation (5), which gives the lateral distribution of the induced lift on the fuselage due to a single pair of horseshoe vortices at $(x_n', \pm y_n')$ and their images, can be written

$$\frac{\Delta\left(\frac{dL_f}{dy}\right)}{q\bar{c}} = \frac{2}{\pi}\left(\frac{cc_l}{\bar{c}}\right)_n \left[\tan^{-1} \frac{2(y_n' - s')\sqrt{1 - y'^2}}{(y_n' - s')^2 - 1} - \tan^{-1} \frac{2(y_n' + s')\sqrt{1 - y'^2}}{(y_n' + s')^2 - 1}\right] \tag{B4}$$

The total lift at a station $\pm y'$ on the fuselage is then

$$\frac{dL_f}{q\bar{c}} = \frac{2}{\pi} \sum_{n} \left(\frac{cc_l}{\bar{c}}\right)_n \left[\tan^{-1} \frac{2(y_n' - s')\sqrt{1 - y'^2}}{(y_n' - s')^2 - 1} - \tan^{-1} \frac{2(y_n' + s')\sqrt{1 - y'^2}}{(y_n' + s')^2 - 1}\right] \tag{B5}$$

The value of $\frac{dL_f/dy}{q\bar{c}}$ at $\pm y' = 0.25$ is calculated from the values in the following table (the lateral lift at any station $\pm y'$ can be calculated in a similar manner):

	(I)	(II)	
n	$\tan^{-1}\frac{2(y_n' - s')\sqrt{1 - y'^2}}{(y_n' - s')^2 - 1}$	$\tan^{-1}\frac{2(y_n' + s')\sqrt{1 - y'^2}}{(y_n' + s')^2 - 1}$	$\left(\frac{cc_l}{\bar{c}}\right)_n\left(\text{(I)} - \text{(II)}\right)_n$
1	1.571	0.918	0.241
2	.918	.633	.104
3	.633	.481	.054
4	.481	.387	.032
5	.387	.324	.020
6	.324	.279	.014
7	.279	.244	.010
8	.244	.217	.007
9	.217	.195	.005
			$\sum = 0.487$

Thus, at $y' = 0.25$,

$$\frac{dL_f/dy}{q\bar{c}} = \frac{2}{\pi}(0.487) = 0.310$$

The complete lateral lift distribution is shown in figure 10.

REFERENCES

1. Multhopp, H.: Aerodynamics of the Fuselage. NACA TM 1036, 1942.

2. Schlichting, H.: Calculation of the Influence of a Body on the Position of the Aerodynamic Centre of Aircraft With Sweptback Wings. Tech. Note No. Aero. 1879, British R.A.E., Mar. 1947.

3. Lennertz, J.: Beitrag zur theoretischen Behandlung des gegenseitigen Einflusses von Tragfläche und Rumpf. Z.f.a.M.M., Bd. 7, Aug. 1927, pp. 249-276.

4. Flax, A. H.: Integral Relations in the Linearized Theory of Wing-Body Interference. CAL - 45, Cornell Aero. Lab., Inc., Nov. 1952.

5. Vandrey, F.: Zur theoretischen Behandlung des gegenseitigen Einflusses von Tragflügel und Rumpf. Luftfahrtforschung, Bd. 14, Lfg. 7, Sept. 7, 1937, pp. 347-355.

6. Young, A. D., and Owen, P. R.: A Simplified Theory for Streamline Bodies of Revolution, and Its Application to the Development of High-Speed Low-Drag Shapes. R. & M. No. 2071, British A.R.C., 1943.

7. Zlotnick, Martin: A Theoretical Investigation of the Effects of the Fuselage on the Spanwise Lift Distribution of a Wing. M. S. Thesis, Univ. of Va., 1951.

8. Diederich, Franklin W.: A Simple Approximate Method for Calculating Spanwise Lift Distributions and Aerodynamic Influence Coefficients at Subsonic Speeds. NACA TN 2751, 1952.

9. Robinson, Samuel W., Jr., and Zlotnick, Martin: A Method for Calculating the Aerodynamic Loading on Wing—Tip-Tank Combinations in Subsonic Flow. NACA RM L53B18, 1953.

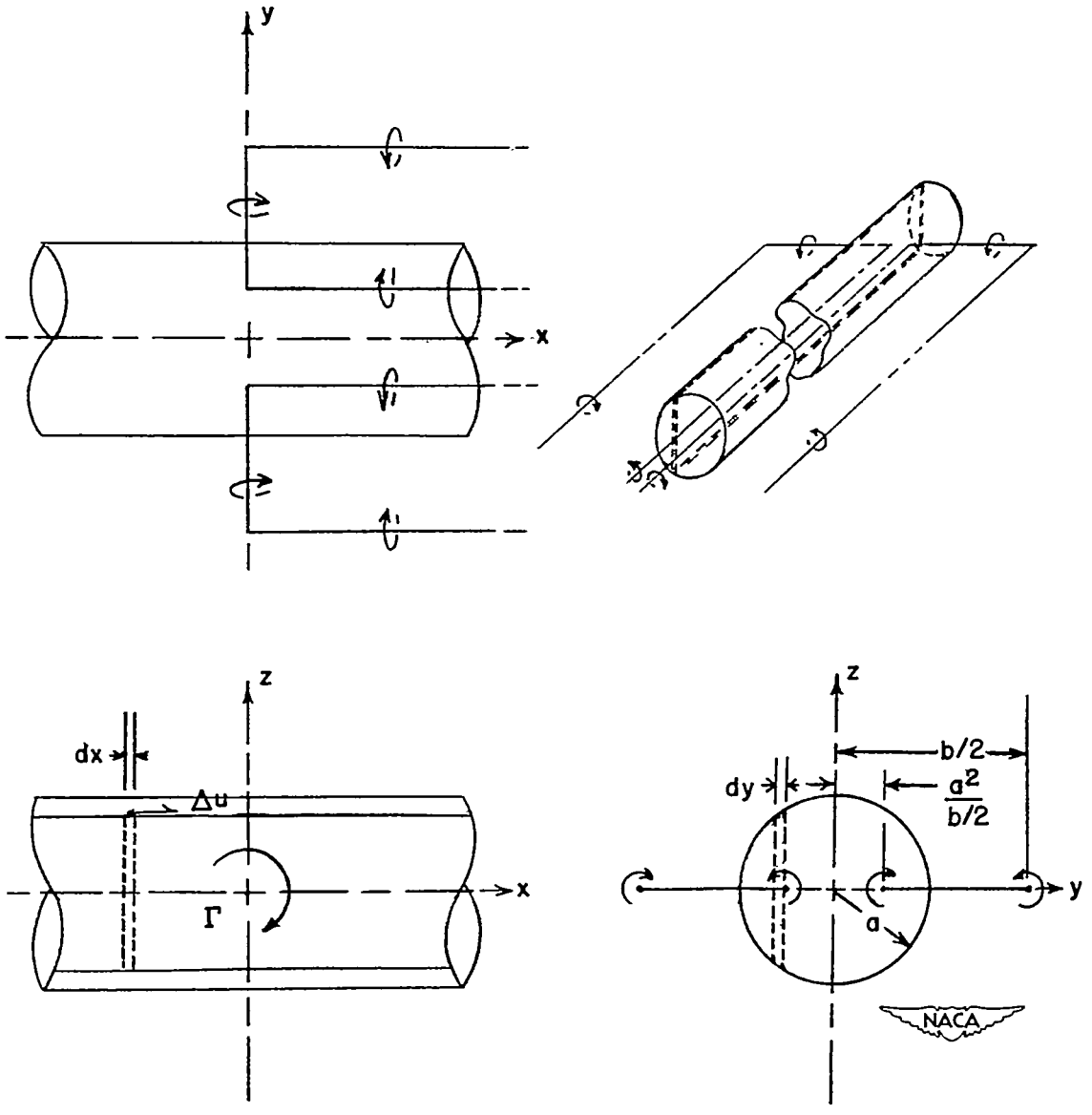

Figure 1.- Combination of horseshoe vortex and infinite cylinder.

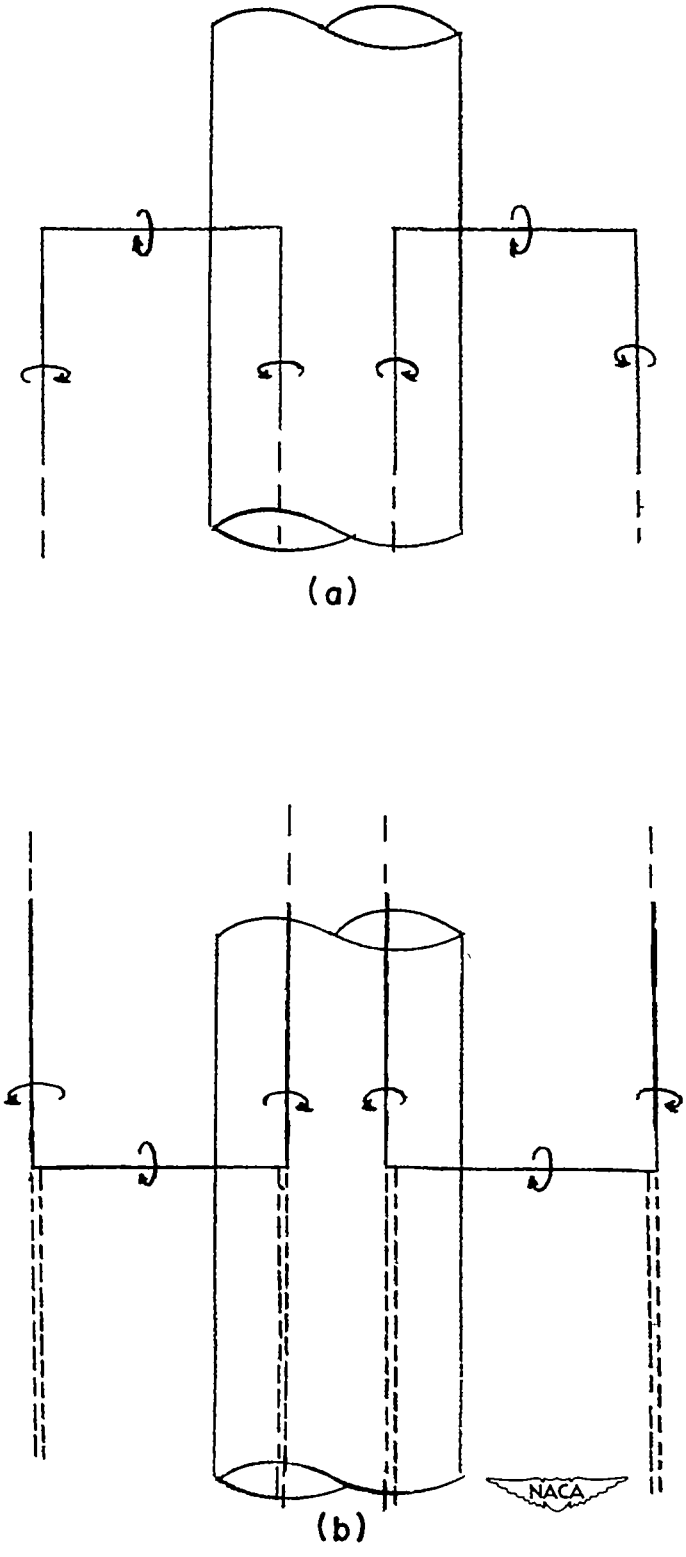

Figure 2.- Illustration showing superposition of infinite trailing vortices on cylinder and horseshoe-vortex system.

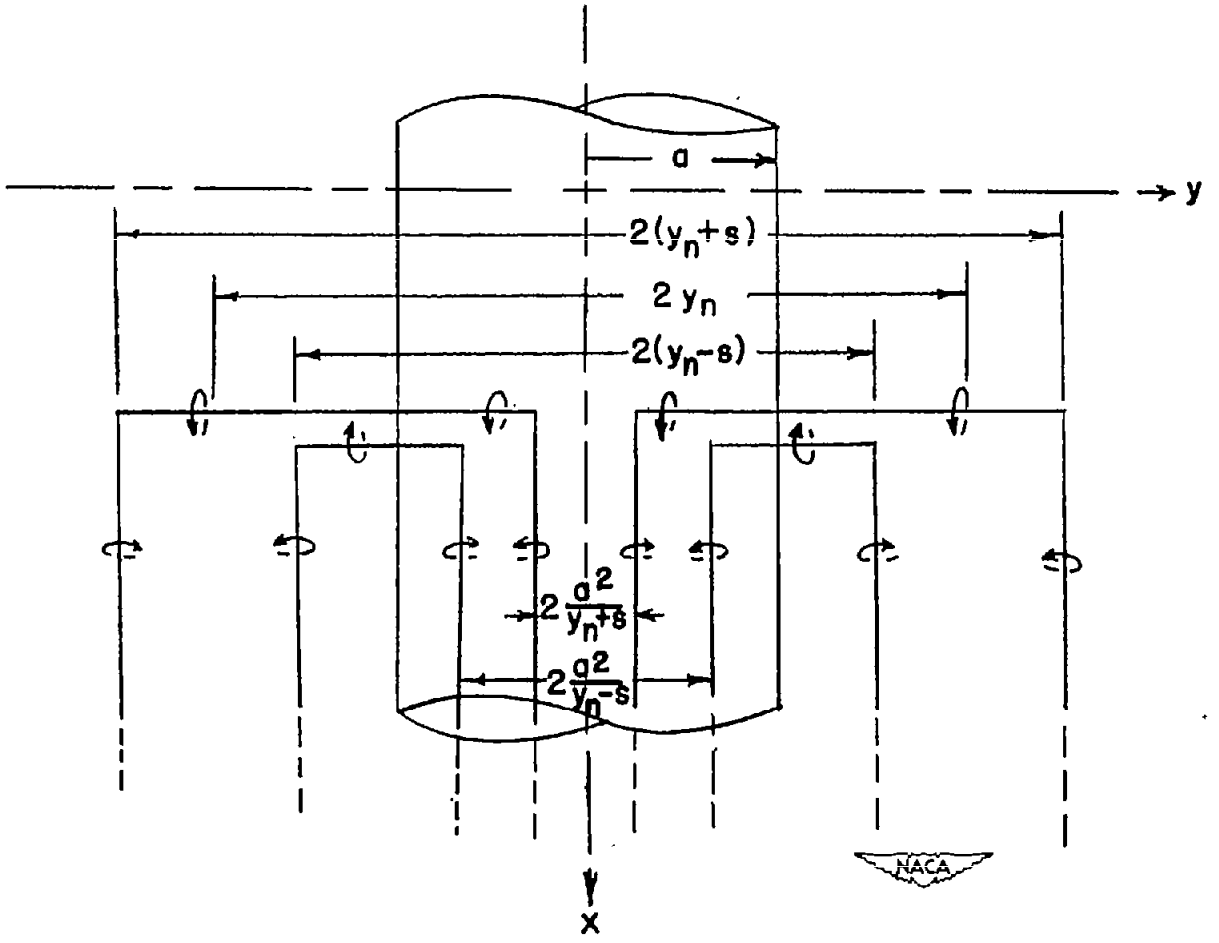

Figure 3.- Superposition of two unequal pairs of symmetrical horseshoe vortices to form a system of discrete horseshoe vortices and their images.

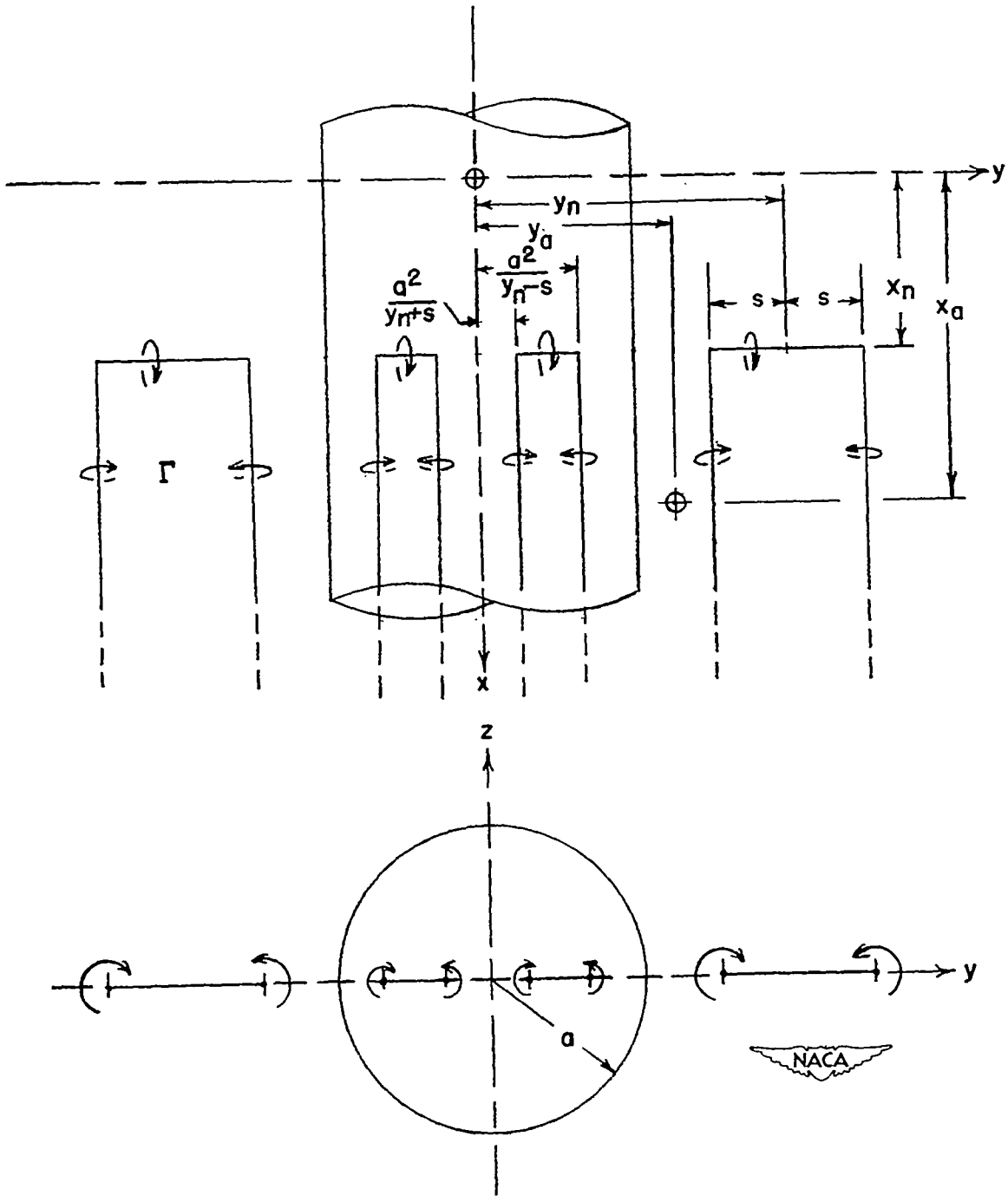

Figure 4.- Cylinder with a pair of symmetrically disposed horseshoe vortices and their images.

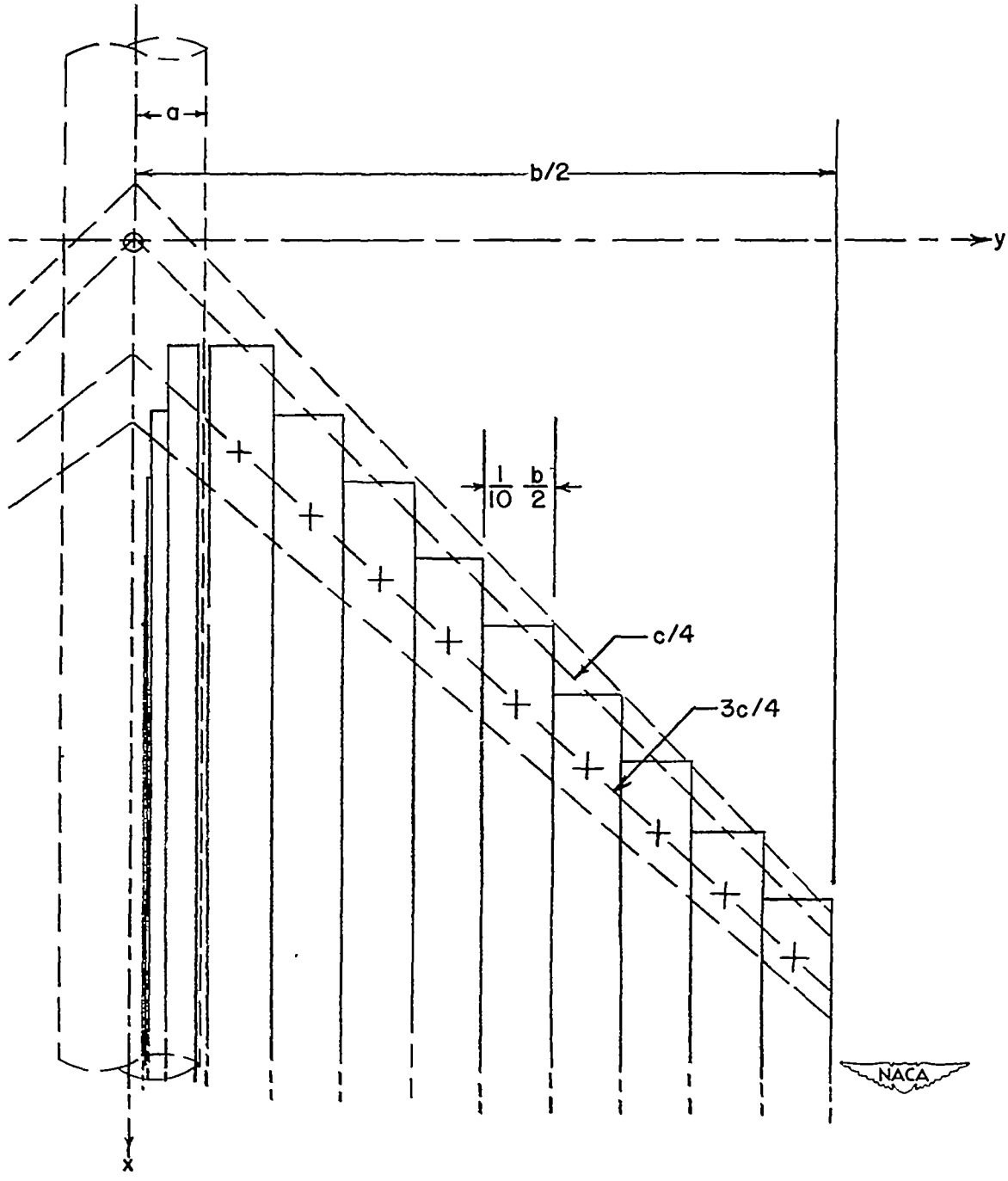

Figure 5.- Cylinder-wing combination. Sweepback angle, 45°; taper ratio, 0.45; A = 8; $a^* = 0.10$.

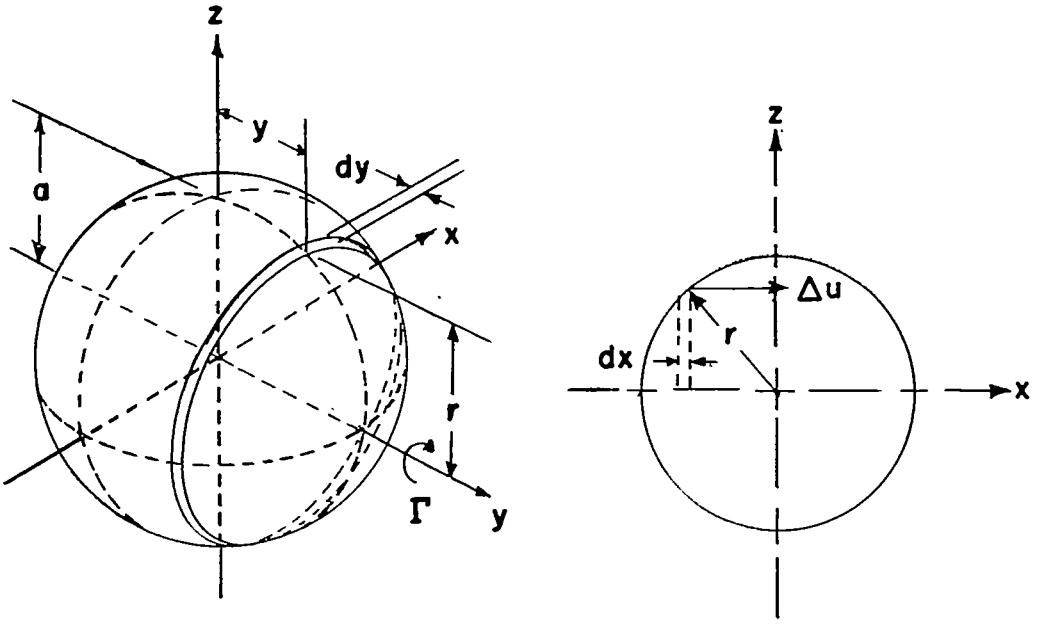

(a) Infinite-vortex—sphere configuration.

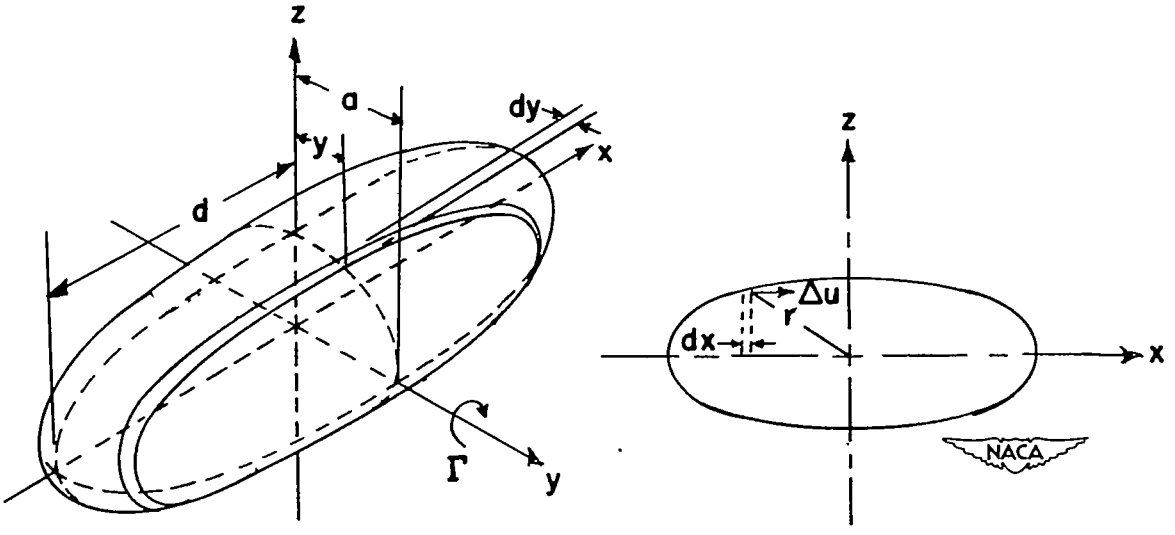

(b) Infinite-vortex—ellipsoid configuration.

Figure 6.- Illustrations of sphere with infinite vortex and ellipsoid with infinite vortex.

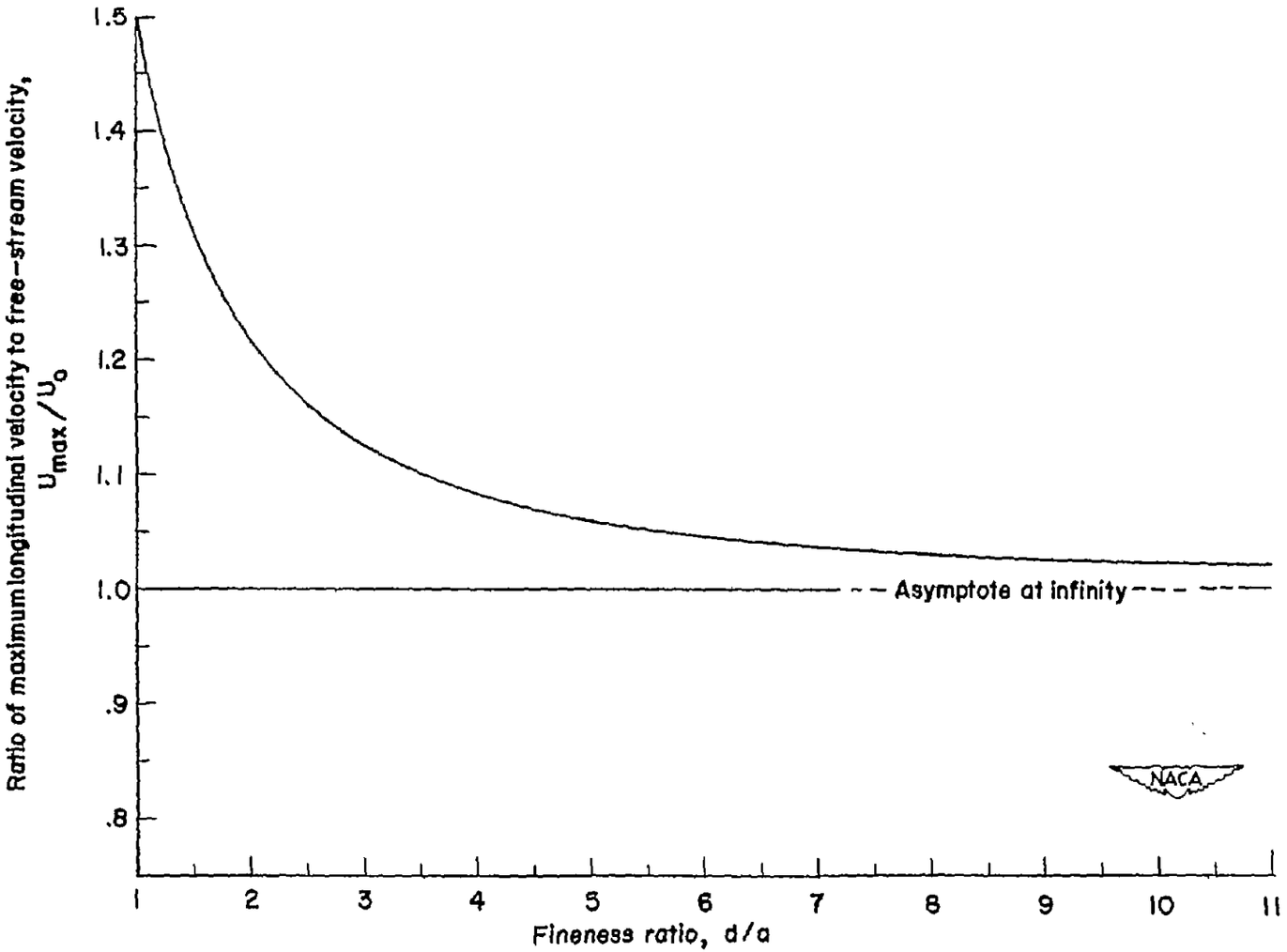

Figure 7.- Effect of fineness ratio on the maximum velocity of flow past an ellipsoid of revolution.

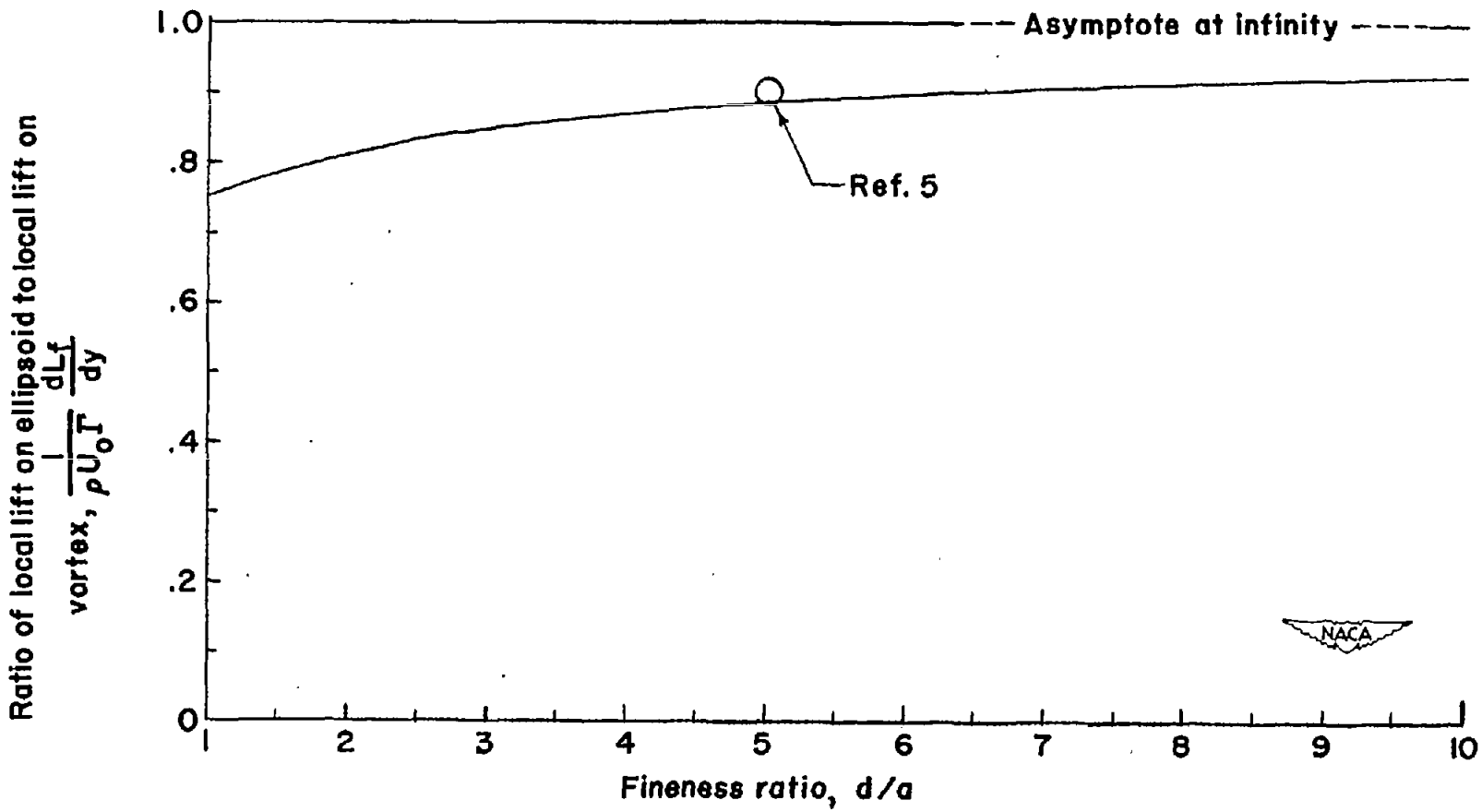

Figure 8.- Effect of fineness ratio on the lift on an ellipsoid of revolution intersected by an infinite vortex having the strength Γ.

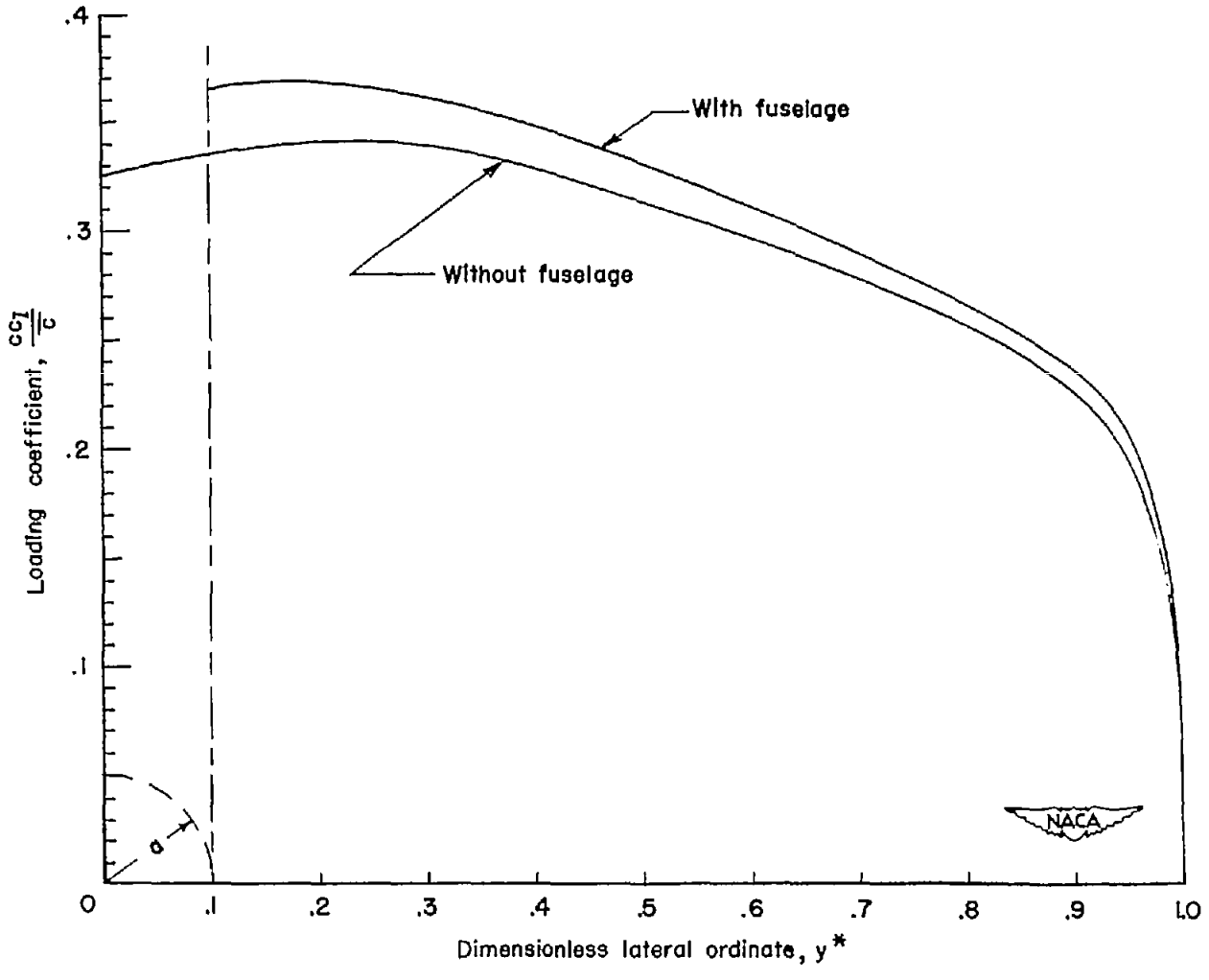

Figure 9.- Lateral lift distribution on the wing alone and on a wing-fuselage combination. Sweepback angle, 45°; taper ratio, 0.45; A = 8; a* = 0.10.

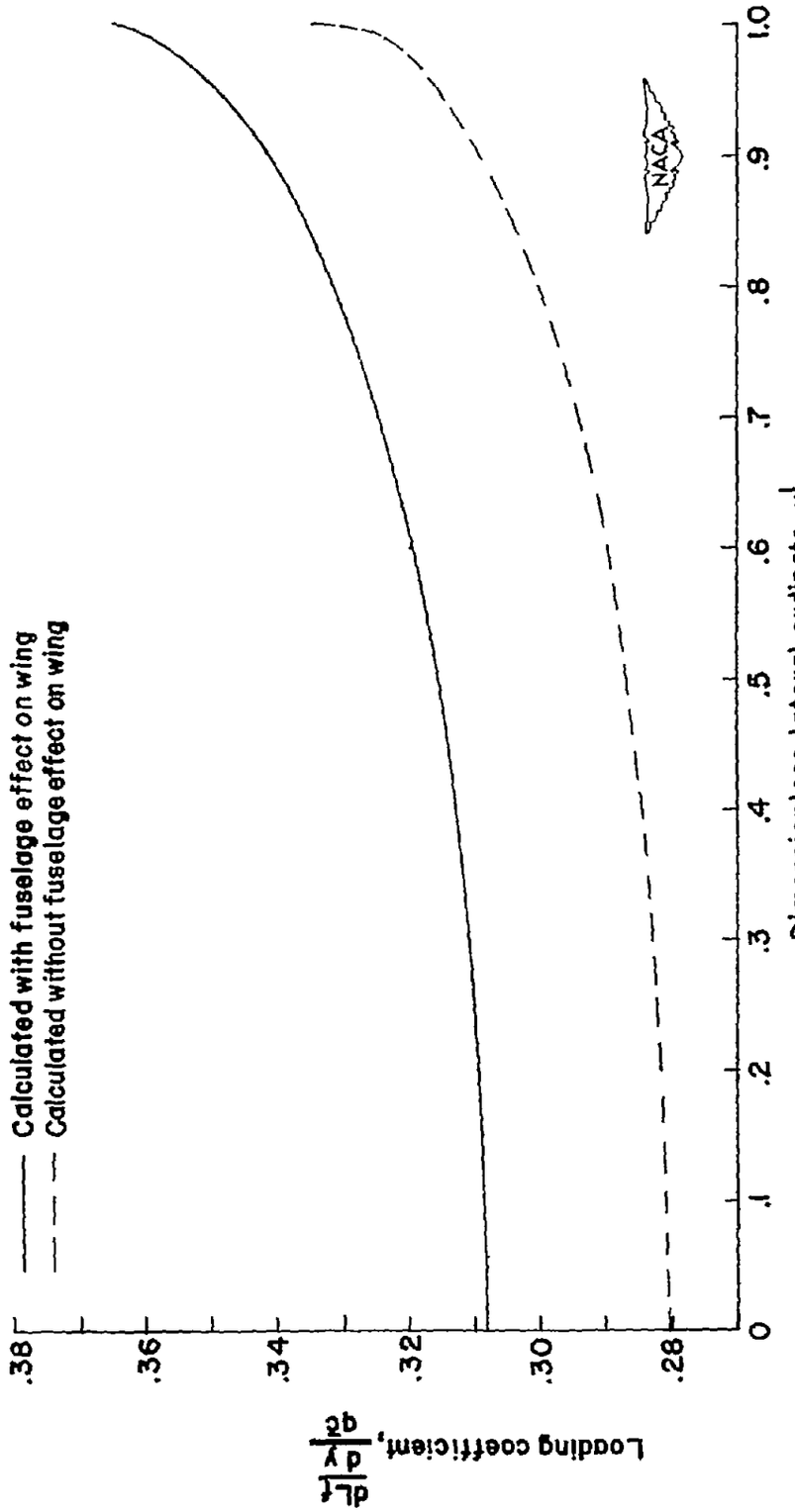

Figure 10.- Lateral distribution of induced lift on the fuselage in the presence of the wing. Sweepback angle, 45°; taper ratio, 0.45; A = 8; a* = 0.10.

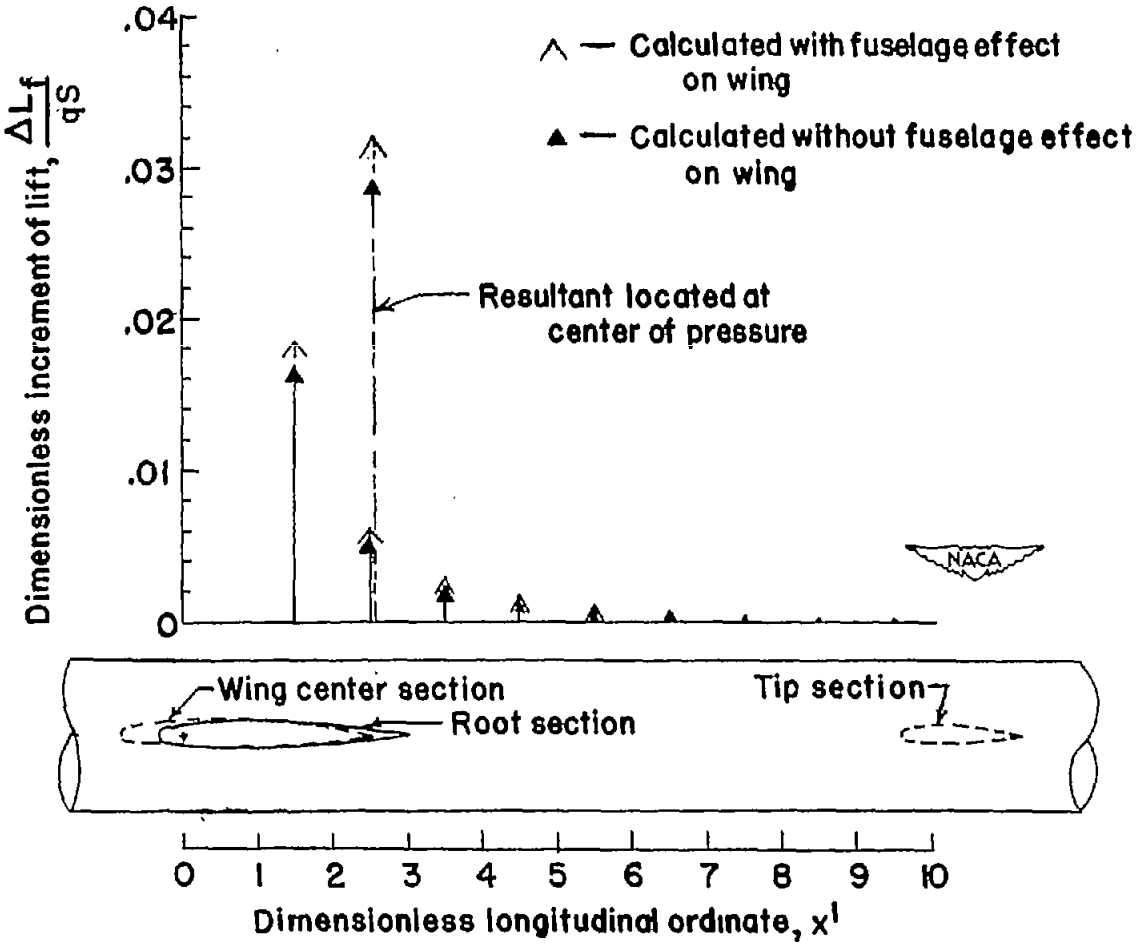

Figure 11.- Longitudinal distribution of induced lift on the fuselage in the presence of the wing. Sweepback angle, 45°; taper ratio, 0.45; A = 8; a* = 0.10.

NACA-Langley - 1-6-54 - 1000